Search for OB associations in Gaia Early Data Release 3

Author: Alexander A. Chemel, Richard de Grijs, Elena V. Glushkova and Andrey K. Dambis

Reporter: Yanan Cao

1. Introduction

- Majority of stars with masses > 0.5 $M_{\odot}$ are formed in groups *(Lada & Lada 2003)*, OB associations are among the main object types through which one can trace active star formation in the Galaxy.
- It is important to study the associations' kinematic and spatial structure and substructure *(Lim et al. 2019)*, as well as of the kinematics of their expansion and determination of their ages.
- The Gaia data release provided more precise information on the parallax and proper motion of about 1.5 billion stars in our Galaxy. This made it possible to establish that OB associations are not a product of the disruption of initially bound stellar aggregations as a result of gas swept out by young stars, as was previously thought *(Hills 1980; Brown, Dekker & de Zeeuw 1997; Kroupa, Aarseth & Hurley 2001; Goodwin & Bastian 2006; Baumgardt & Kroupa 2007)*, but they are born unbound and inherit the kinematic and structural properties of their parent giant molecular clouds *(Wright & Mamajek 2018; Ward & Kruijssen 2018; Lim et al. 2019; Ward, Kruijssen & Rix 2020)*. Thus, the density spectrum of stellar groups is continuous *(Allen et al. 2007; Evans et al. 2009; Lamb et al. 2010)*, and modern OB associations are not necessarily subject to global expansion *(Mel'nik & Dambis 2017; Melnik & Dambis 2020)*.

2. The Sample

❑In order to search for OB associations, they compiled a sample which included not only O- and early B-type stars (with masses ≥20 $M_\odot$) but also young OCs.

- a list of 72 550 OB stars from the Skiff (2014) catalogue of spectral classifications

- OB stars from LAMOST DR5 and Xu et al. (2018)(provided information about an additional 10 482 objects)

- 1743 OCs from the Dias et al. (2021) catalogue(based on Gaia DR2 data)

❑Restrictions include: (i) $|b| < 20°$; (ii) only 955 young OCs(log t (yr) ≤ 8.3); (iii) $N_{per} > 8$ and RUWE < 1.25

→The result was a sample of 47 735 objects, including 46 780 OB stars from various sources and 955 young OCs.

2. The Sample

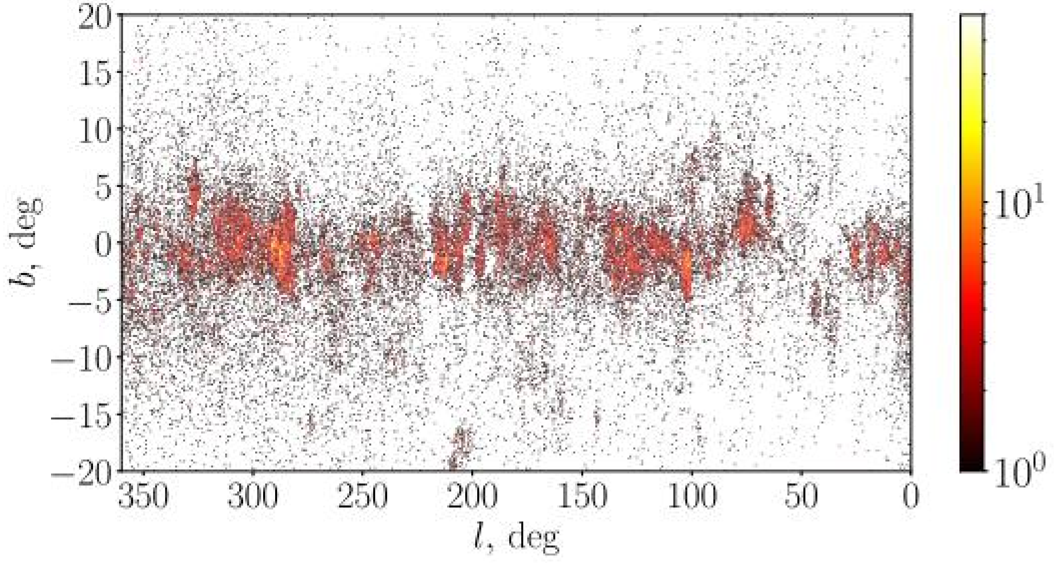

Figure 2. Distribution of our sample objects on the sky in Galactic coordinates. The colour scale corresponds to the logarithm of their density.

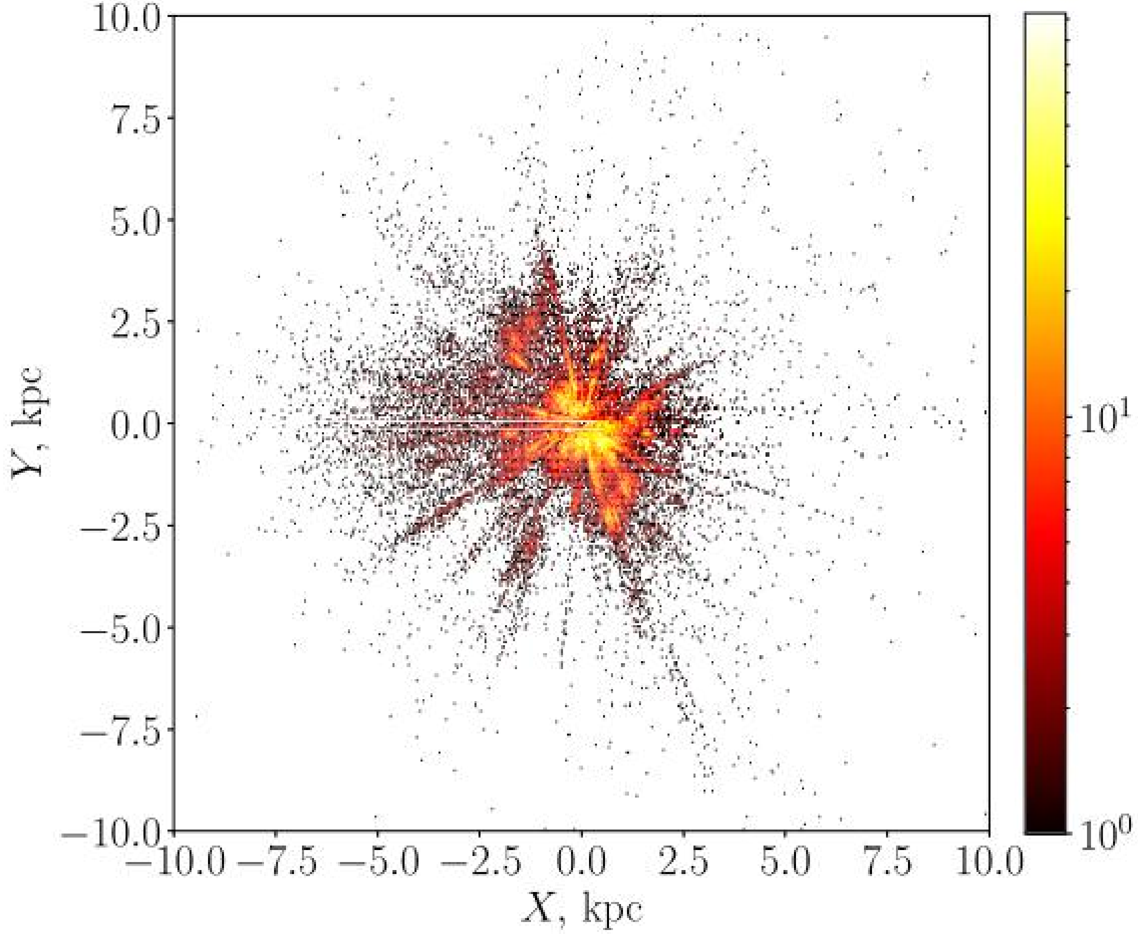

Figure 3. Distribution of our sample objects in the Galactic symmetry plane. The colour scale corresponds to the logarithm of their density. The x-axis is directed to the centre of the Galaxy, the y-axis is in the direction of Galactic rotation.

4. Results

- They excluded radial velocities from consideration at the clustering stage, limiting their phase space to five dimensions: two stellar proper motion components, (PM_α, PM_δ) , and three coordinates (X, Y, Z).
- They use HDBSCAN* for clustering and set *min_cluster_size* = 10.

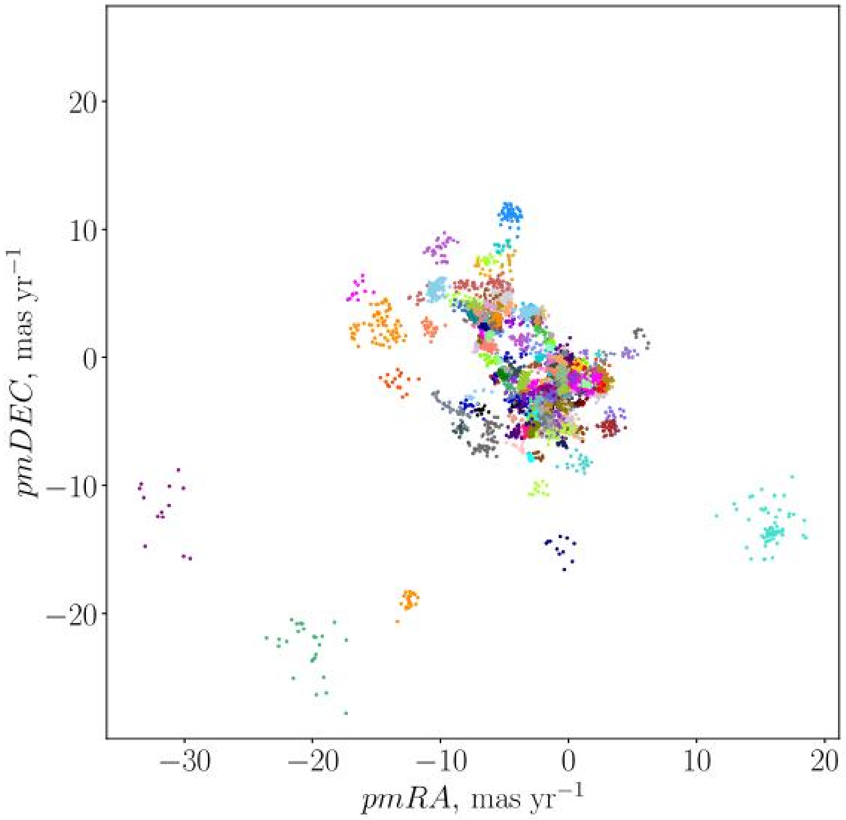

Figure 5. Clustering result for *min_cluster_size* = 10 in proper-motion space. All 214 clusters are plotted using random colours.

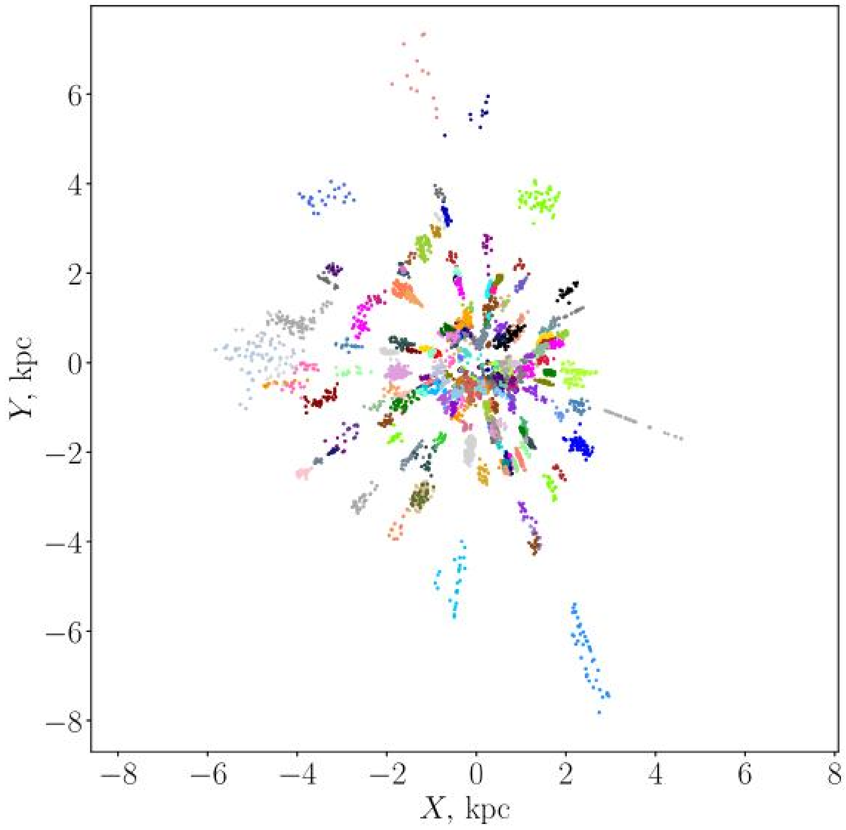

Figure 6. As Fig. 5, but projected on to the Galactic plane. The colours correspond to the ones of the clusters in the Fig. 5. The Galactic Centre is on the right. The origin of coordinates corresponds to the position of the Sun.

4. Results

- Method: Monte Carlo
- $PM_j = k_j(j - j_0) + c_j$, where $j = (l, b)$.
- Inverse velocity gradients provide an estimate of the kinematic age of a cluster, i.e. the period during which the expansion occurred.
- Kinematic ages $= \frac{1}{k}$

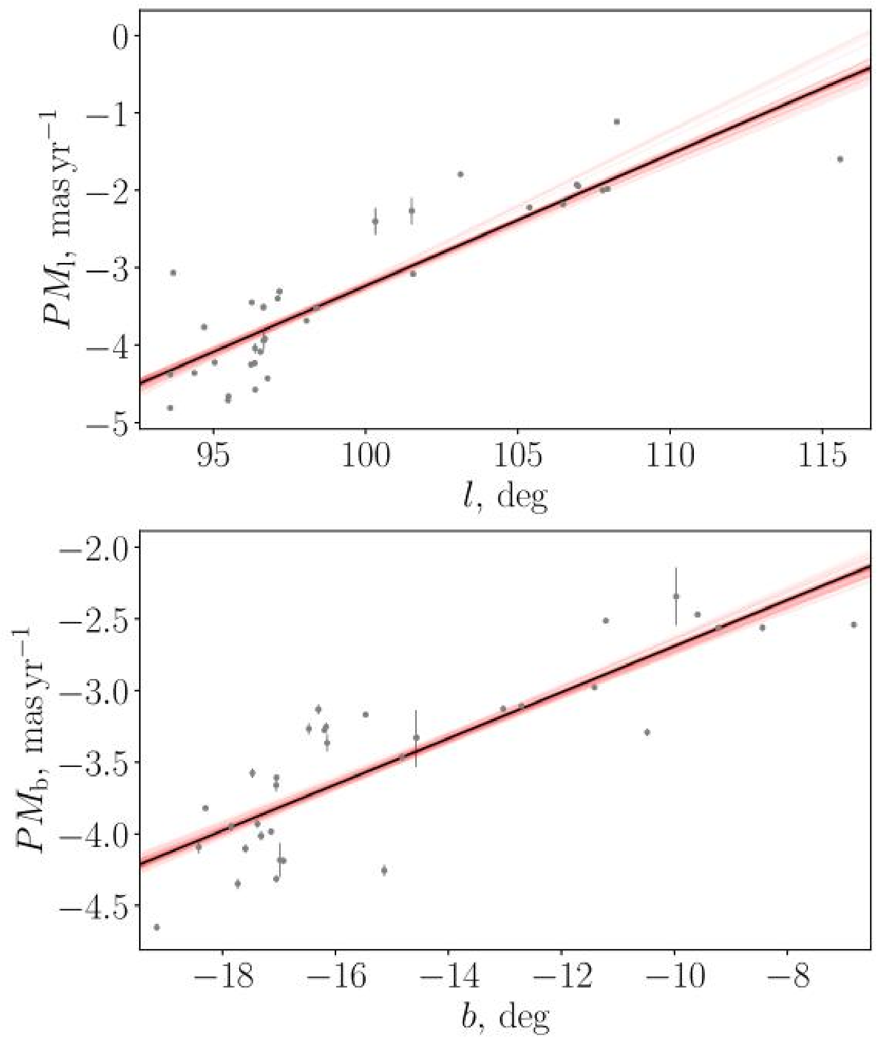

Figure 7. (Top) (PM_l, l) diagram for cluster no. 44. (Bottom) (PM_b, b) diagram for the same cluster. Straight black lines represent linear fits for median kinematic ages of 21.15 ± 0.27 Myr and 22.37 ± 0.42 Myr for the top and bottom panels, respectively. The red solid lines show the spread of the results of the least-squares method from all 100 iterations.

4. Results

- ❑Student's t -test: to control the quality of the correlations between proper motions and the corresponding coordinates.

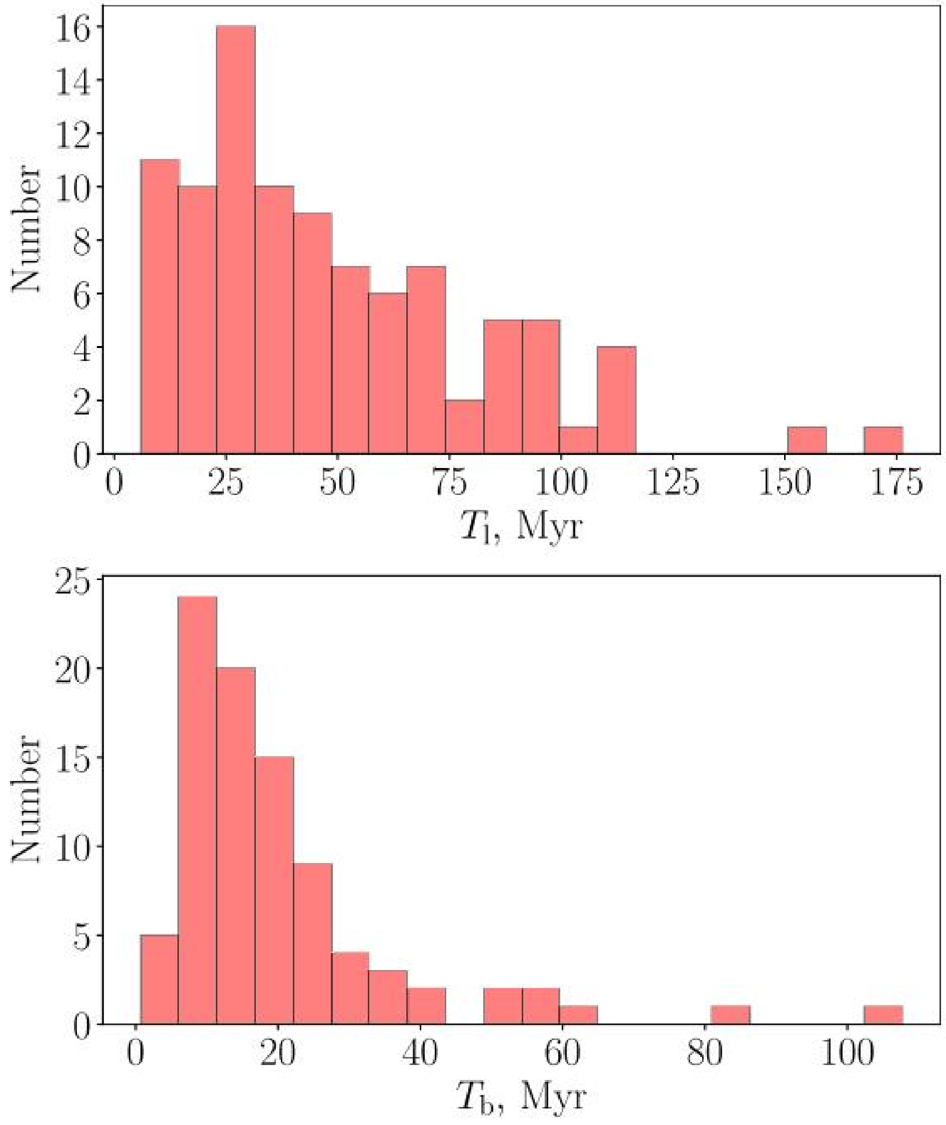

Figure 8. Distribution of ages obtained from 'proper motion–coordinate' diagrams for Galactic longitude (top) and latitude (bottom) for clusters that satisfied the Student's t test at the 1σ confidence level.

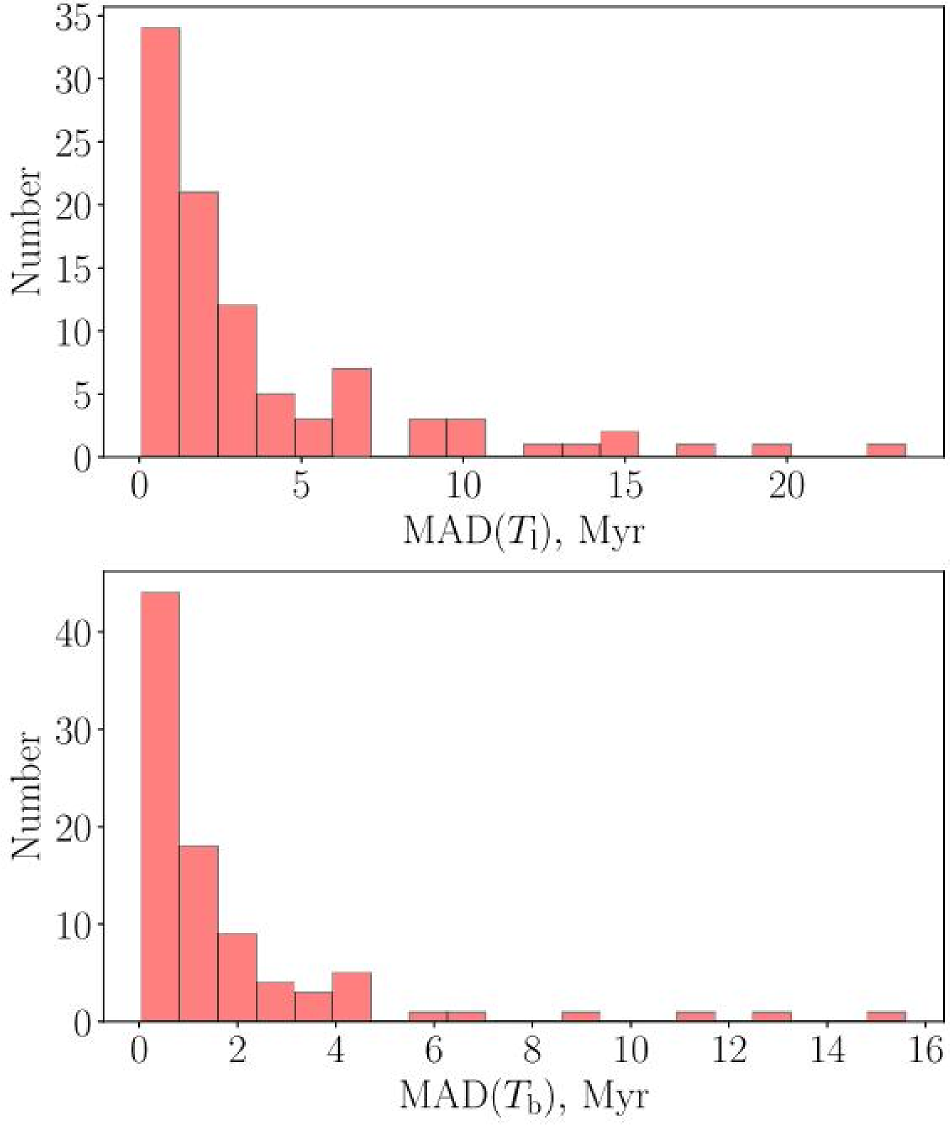

Figure 9. As Fig. 8, but for the age uncertainties, defined as MAD.

4. Results

- ❑The first peak (−0.3 ≤ ξ ≤−0.15): a part of the Inner arm
- ❑The second peak (−0.15 ≤ ξ ≤ 0.02) : the Carina–Sagittarius (Car–Sag) arm
- ❑The third (0.02 ≤ ξ ≤ 0.22) and small fourth (0.22 ≤ ξ ≤ 0.4) peaks: the Perseus arm region
- ❑The depressions at ξ ≈−0.15 and ξ ≈ 0.03: coincide with the interarm intervals

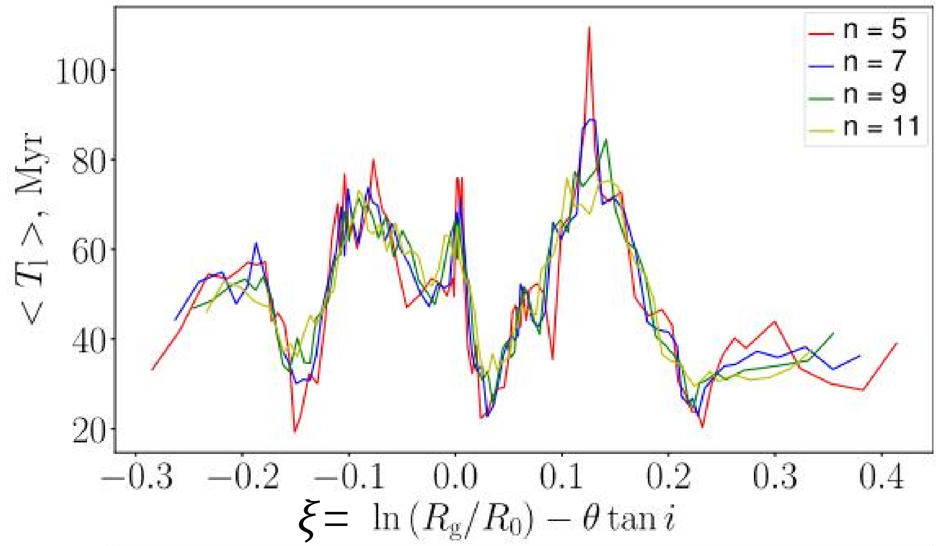

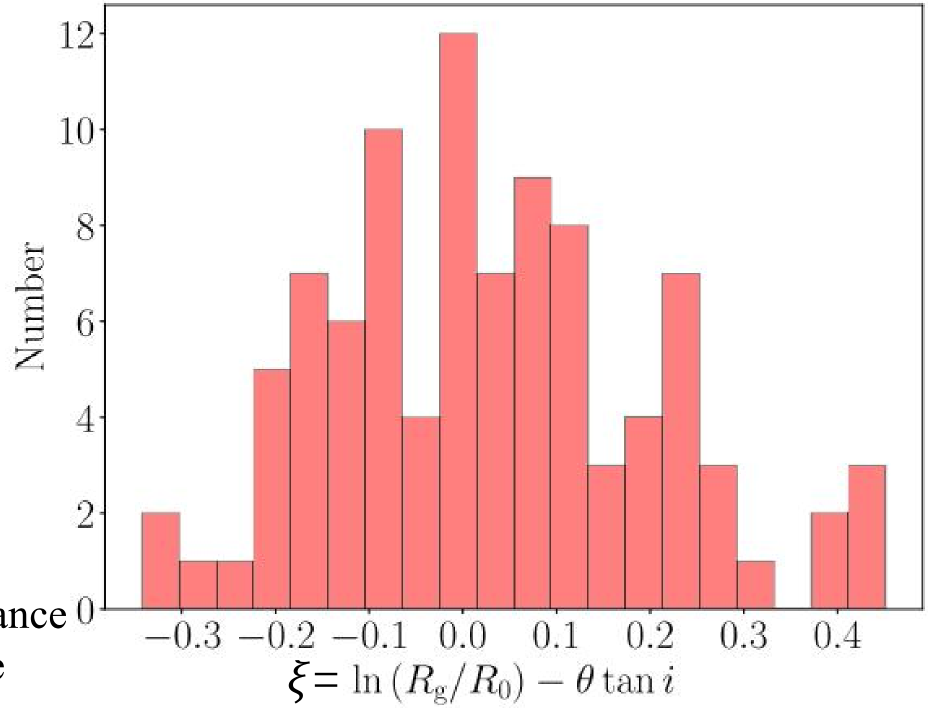

ξ parameter: instead of the Galactocentric distance
R_0 = 8210 pc: the solar Galactocentric distance
θ: Galactocentric azimuth
i = −10.4° : the pitch angle of the spiral pattern.

Conclusion

- They compiled a well-defined sample of OB stars based on the LAMOST DR5 (Zhao et al. 2012), Xu et al. (2018), and Skiff (2014) catalogues, supplemented with young OCs from Dias et al. (2021). The resulting sample contains more than 47 700 young objects located in the Galactic thin disc.
- They used the HDBSCAN* algorithm and set the parameter *min_cluster_size* = 10 and found 214 clusters.
- They investigated the proper motion–coordinate diagrams along Galactic longitude and latitude for all clusters using the Monte Carlo method, and they obtained kinematic age in clusters.
- The dependence of the mean age on Galactocentric distance and on the parameter $\xi = \ln\left(R_g/R_0\right) - \theta \tan(i)$ demonstrated a correlation between the positions of peaks and depressions with Galactic spiral arms. The positions of local peaks, marking areas of increased mean age, correlate with the position of the Inner , Car–Sgr , and Perseus arms.